

# Probing of Cardiomyocyte Metabolism by Spectrally Resolved Lifetime Detection of NAD(P)H Fluorescence

S Aneba<sup>1</sup>, Y Cheng<sup>1</sup>, A Mateasik<sup>2</sup>, B Comte<sup>1,3</sup>,  
D Chorvat Jr<sup>2</sup>, A Chorvatova<sup>1,4</sup>

<sup>1</sup>Research Centre, CHU Sainte-Justine, Montreal, Canada

<sup>2</sup>International Laser Centre, Bratislava, Slovakia

<sup>3</sup>Department of Nutrition, University of Montreal, Montreal, Canada

<sup>4</sup>Department of Pediatrics, University of Montreal, Montreal, Canada

## Abstract

*NAD(P)H, crucial in effective management of cellular oxidative metabolism and the principal electron donors for enzymatic reactions, is a major source of autofluorescence induced in cardiac cells following excitation by UV light. Spectrally-resolved time-correlated single photon counting was used to simultaneously measure the fluorescence spectra and fluorescence lifetimes of NAD(P)H, following excitation by a pulsed picosecond 375 nm laser diode. Spectra, as well as fluorescence lifetimes of NADH and NADPH molecules were investigated in solution at different concentrations. Effects of their respective dehydrogenation by lipoamide dehydrogenase (LipDH) or glutathione reductase (GR) were also questioned. NAD(P)H autofluorescence recorded in vitro was compared to the one measured in freshly isolated cardiac cells. We observed a good comparability between NAD(P)H parameters recorded in solution and in cells.*

## 1. Introduction

Endogenous fluorescence of NAD(P)H, induced following excitation with the UV light, is long used for non-invasive fluorescent probing of metabolic state. Blue autofluorescence of rat cardiac myocytes was demonstrated to correlate with metabolic changes and was mostly ascribed to mitochondrial NADH and NADPH [2]. Adenosine triphosphate (ATP), produced in the process of mitochondrial oxidative phosphorylation, is the primary molecular energy source for the contraction of cardiac myocytes. This process is coupled to oxidation of reduced NADH, the principal electron donor for the electrochemical gradient indispensable for oxidative energy metabolism. The first step in this process, which accounts for 95% of ATP

generation needed for cardiomyocyte contraction, is the dehydrogenation of NADH by Complex I of the mitochondrial respiratory chain. NADH consumption rate is long investigated using fluorescence techniques in tissues and isolated mitochondria. On the other hand, NADPH is an important cofactor for several enzymes involved in different metabolic pathways (i.e. pentose phosphate pathway, Krebs cycle) and is essential for antioxidant processes in the glutathione reductase (GR) reaction. This enzyme allows the recycling of glutathione by converting its oxidized form (GSSG) into reduced glutathione. Oxidative stress can modulate the cellular NADPH content through the release of peroxides and various by-products that has been shown to decrease the activity of several enzymes, such as the NADP-isocitrate dehydrogenase (NADP-ICDH) [1]. Here, we investigate NAD(P)H fingerprinting by spectrally-resolved lifetime spectroscopy. More precisely, we characterize fluorescence spectra and fluorescence lifetimes of NADH and NADPH in intracellular-like solutions and compare resolved data with spectral and temporal characteristics of endogenous NAD(P)H fluorescence, directly in living cardiomyocytes.

## 2. Methods

### 2.1. Cardiomyocyte isolation

Left ventricular myocytes were isolated from Sprague-Dawley rats (13-14 weeks old, Charles River, Canada) following retrograde perfusion of the heart with proteolytic enzymes [4]. All procedures were performed in accordance with Institutional Committee accredited by the Canadian Council for the Protection of Animals (CCPA). Myocytes were maintained in a storage solution at 4°C until used. Only cells that showed clearly defined striations were used in up to 10 hrs following isolation.

## 2.2. TCSPC

We have used time correlated single photon counting (TCSPC) setup based on inverted microscope (Axiovert 200M, Zeiss, Canada) [4]. In brief, a picosecond diode laser with emission line at 375 nm (BHL-375, Becker-Hickl, Boston Electronics, USA) was used as an excitation source (output power  $\sim 1$  mW, repetition rate 20 MHz, pulse widths typically  $< 100$  ps). The laser beams were combined by dichroic filters and reflected to the sample through epifluorescence path of Axiovert 200 inverted microscope to create slightly defocused elliptical spot (10-20  $\mu\text{m}$ ). The emitted fluorescence was spectrally decomposed by 16-channel photomultiplier array (PML-16, Becker-Hickl, Boston Electronics, USA), running in the photon-counting regime and feeding the time-correlated single photon counting interface card SPC 830 using SPCM software (both Becker-Hickl, Boston Electronics, USA), attached to the imaging spectrograph (Solar 100, Proscan, Germany). Fluorescence decays were measured for 30 s with 25 ns TAC time-base sampled by 1024 points. Cells were studied at room temperatures in 4-well chambers with UV-proof coverslip-based slides (LabTech).

## 2.3. Solutions, drugs and data analysis

The basic external solution contained (in mM): NaCl, 140; KCl, 5.4;  $\text{CaCl}_2$ , 2;  $\text{MgCl}_2$ , 1; glucose, 10; HEPES, 10; adjusted to pH 7.35 with NaOH. Basic intracellular solution contained (in mM): KCl, 140; NaCl, 10; glucose, 10; HEPES, 10; adjusted to pH 7.25 with NaOH. LipDH (porcine; 2 U/ $\mu\text{L}$ ), NADH or NADPH in concentrations ranging from 1 to 20  $\mu\text{M}$  were added to basic internal solution. NADPH was also produced from NADP-ICDH (3.9 U/mL) by reaction of Isocitrate (89 mM) and NADP (0.5 mM) with or without GSSG (50 nM) and GR (0.5 U/mL or 1 U/mL). Chemicals were from Sigma-Aldrich (Canada). Data were analyzed using SPCImage software (Becker-Hickl, Boston Electronics, USA), Origin 7.0 (OriginLab, USA) and custom-written procedures for data correction and analysis written in C++. Home-made database was used for appropriate data management. Data are shown as means  $\pm$  standard errors (SEM).

## 3. Results

### 3.1. NADH and NADPH in vitro

Fluorescence spectra and fluorescence lifetimes of intrinsic NADH and NADPH fluorescence were recorded in vitro in intracellular media-mimicking solutions. Steady-state emission spectra measured simultaneously at

16 acquisition channels were determined as the total photon counts on each spectral channel. Concentrations ranging from 1 to 20  $\mu\text{M}$  were used to question the dose dependence of spectral and lifetime properties of the NADH and NADPH fluorescence. Spectral intensity of NADH fluorescence followed linear concentration-dependence (Fig. 1A), as described previously [2].

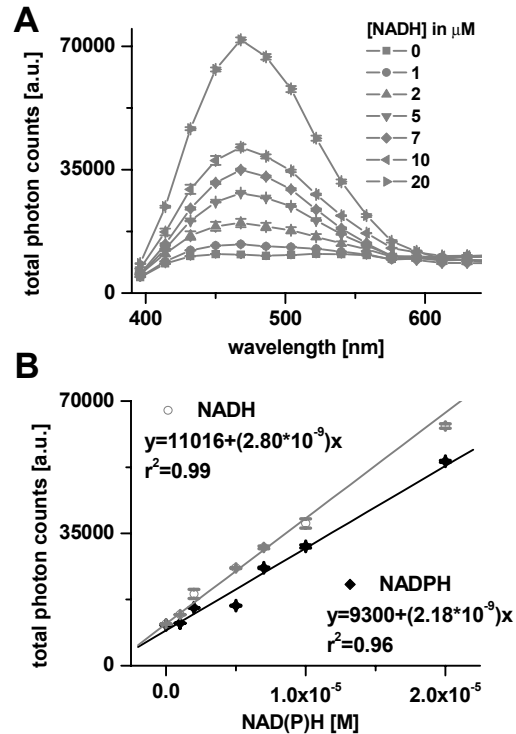


Figure 1. Emission spectra of NADH *in vitro* in intracellular solutions at concentrations ranging from 1 to 20  $\mu\text{M}$  ( $n=5$  samples each) (A). Concentration-dependence of the NADH and NADPH autofluorescence at spectral peak of 450 nm (B).

Normalized spectra superimposed perfectly for NADH concentrations between 1 to 20  $\mu\text{M}$  (data not shown), confirming the same molecular origin. Free NADPH and NADH had autofluorescence with spectral maximum at 450 and 470 nm respectively in intracellular solution (Fig. 4). The spectral intensity of NADPH/NADH was linearly dependent on their concentration, as illustrated in Fig. 1B at 450 nm. Quantum yield of NADPH was smaller than that of NADH, as previously reported [2]. Normalized fluorescence intensity recorded in intracellular medium showed slight shift of about 20 nm between NADPH and NADH (Fig. 4). At the fluorescence maximum wavelength of 450 nm we have resolved three fluorescence lifetimes for NADH (20  $\mu\text{M}$ ,  $n=10$  samples):  $\tau_1 = 0.39 \pm 0.01$  ns (with relative amplitude of  $69.9 \pm 1.0\%$ ),  $\tau_2 = 1.46 \pm 0.05$  ns ( $20.5 \pm 0.8\%$ ) and  $\tau_3 = 8.12 \pm 0.07$  ns ( $9.8 \pm 0.2\%$ ), but only 2 significant ones for

NADPH (20  $\mu$ M, n=5 samples):  $\tau_1 = 0.31 \pm 0.01$  ns (74.6  $\pm 2.4\%$ ) and  $\tau_2 = 0.75 \pm 0.02$  ns (25.3  $\pm 2.9\%$ ). Resolved lifetime parameters were independent on the studied emission wavelength, or concentrations (data not shown).

### 3.2. NADPH regulation by GR and NADH regulation by LipDH

NADPH produced *in vitro* from NADP-ICDH had same spectral and lifetime characteristics as NADPH in intracellular solution (data not shown). In the presence of GSSG, GR lowered (0.5 U/mL) or nearly completely abolished (1 U/mL) NADPH autofluorescence produced by NADP-ICDH (Fig. 2A), in agreement with dehydrogenation of NADPH by GR. Normalized and blank-corrected spectra showed no difference of NADPH spectral properties in the presence or absence of GR with GSSG and our data revealed no modifications of NADPH lifetime kinetic properties by GR (data not shown).

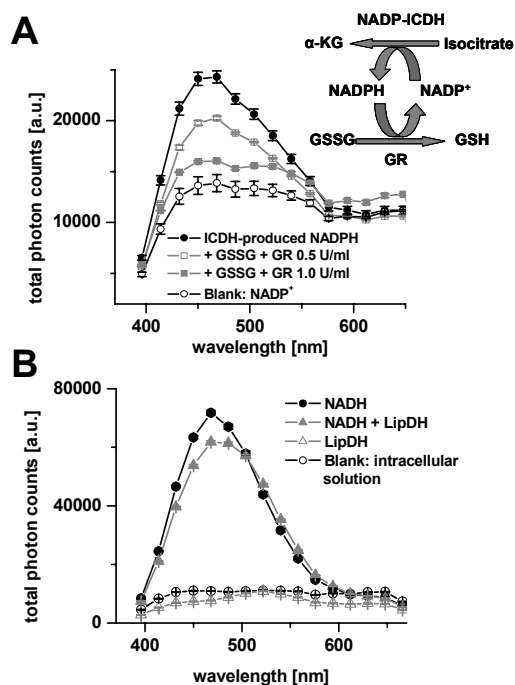


Figure 2. Normalized, background-corrected steady-state emission spectra of ICDH-produced NADPH in the absence and presence of GR (0.5 or 1 U/mL, n=5 samples each) (A) and of 20  $\mu$ M NADH (n=10) in the absence and presence of 2 U/ $\mu$ L LipDH in intracellular solution (n=5) (B).

On the other hand, dehydrogenation of NADH (20  $\mu$ M) to NAD<sup>+</sup> by LipDH (at 2 U/ $\mu$ L) - a disulfide oxidoreductase which is a part of the multienzyme Complex I - decreased fluorescence intensity (Fig. 2B). The effect was accompanied by a spectral broadening of

about 10 nm towards red spectral region, as demonstrated by normalized emission spectra (Fig. 3A). NADH fluorescence decays were prolonged by LipDH (Fig. 3B) due to a significantly increased lifetime of the component 2 (at 504 nm,  $\tau_2$  was prolonged from  $1.84 \pm 0.12$  ns to  $2.74 \pm 0.18$  ns,  $p < 0.05$ ).

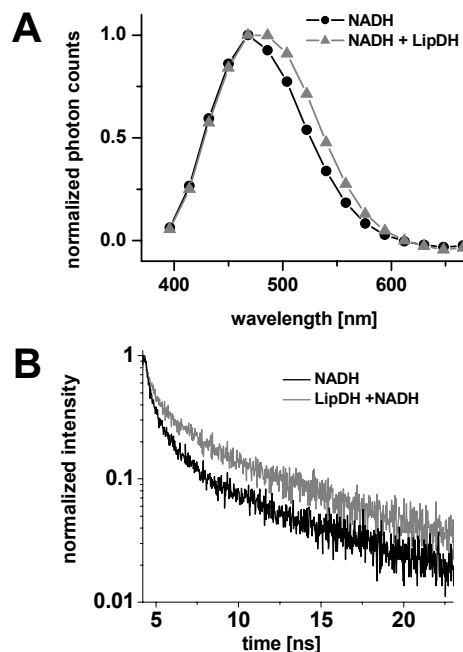


Figure 3. Comparison of normalized, background-corrected steady-state emission spectra of NADH (20  $\mu$ M; n=10 samples) in the absence or presence LipDH (2 U/ $\mu$ L) in intracellular solution (n=5) (A). NADH normalized fluorescence lifetimes (20  $\mu$ M) at 504 nm with or without LipDH (2 U/ $\mu$ L) (B).

### 3.3. Endogenous NAD(P)H in cardiac cells

To investigate the endogenous fluorescence of NAD(P)H in living cardiomyocytes, spectrally and time-resolved autofluorescence decays were recorded in cells bathed in basic external solutions. Normalized steady-state emission spectra of the cardiomyocyte autofluorescence had spectral maximum at 450 nm (Fig. 4) and showed a slight blue-spectral shift when compared to NADH *in vitro*, while being closer to those of NADPH. Analysis of exponential decay of cardiomyocyte autofluorescence showed acceptable chi-square values ( $\chi^2 < 1.2$ ; n=70/13 animals) and flat plot of weighted residuals when using at least a 3-exponential model, namely  $\tau_1 = 0.69 \pm 0.01$  ns (69.3  $\pm 1.0\%$ ),  $\tau_2 = 2.03 \pm 0.05$  ns (27.6  $\pm 0.9\%$ ) and  $\tau_3 = 12.68 \pm 0.08$  ns (3.1  $\pm 0.2\%$ ).

#### 4. Discussion and conclusions

Although spectra of intrinsically fluorescing substances are now well characterized in cardiac tissue, the fluorescence lifetimes, considered to provide better quantitative measurement of different NAD(P)H conformations and/or molecular complexes contributing to the UV-excited autofluorescence of biological samples, are much less clearly identified in living cells. Here we demonstrate that NAD(P)H autofluorescence can be measured in living cardiomyocytes by time-resolved emission spectroscopy approach with good reproducibility. Recorded autofluorescence kinetics were comparable to already published data in cardiac mitochondria [2]. As expected, comparison with NADH and NADPH kinetics *in vitro* pointed to the NAD(P)H origins of the autofluorescence. While our data confirmed close spectral characteristics of NADH and NADPH molecules, curiously, we have identified differences in their lifetimes. This can be due to distinct kinetics of the two molecules, or the presence of impurities; kinetics of further purified molecules need to be done in the future.

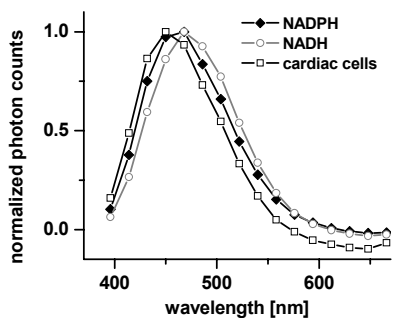


Figure 4. Normalized, background-corrected emission spectra, determined as total photon counts of NAD(P)H autofluorescence of single cardiac cells, compared to NADH and NADPH (both 20  $\mu$ M) in basic extracellular solution.

The LipDH flavoprotein served as example to investigate NADH dehydrogenation. Observed increase in the lifetime kinetics can be related to conformational changes of NADH induced by the enzyme. Indeed, upon dehydrogenation, the oxidized form of the protein promotes the binding of the neutral dihydro-nicotinamide moiety of NADH [3], in addition to the formation of negatively charged charge-transfer complexes between transiently bound  $\text{NAD}^+$  and covalently bound flavin adenine dinucleotide (FAD) cofactor. In this reduced form, nicotinamide moiety is in a different conformation from uniformly ordered structure of NADH juxtaposing nicotinamide and isoalloxazine flavin ring systems and is not proximal to FAD [3], which can be reflected in the

change of fluorescence kinetics. On the other hand, appearance of the red-spectral shoulder points to possible presence of Förster resonant energy transfer (FRET). Being a flavoprotein, excitation of LipDH by visible light (420-460 nm) results in green FAD-autofluorescence with emission maximum around 500 nm [4]. As the LipDH-binding domain for NADH is in close proximity to  $\text{FAD}^+$ -binding one [3] and the 450 nm emission maximum of NADH corresponds exactly to an absorption peak of the  $\text{FAD}^+$  moiety, this fulfils the prerequisites for the FRET between the two molecules. Nevertheless, since no decrease in NADH lifetime(s) was observed, further study is needed to fully understand significance of changes in NADH fluorescence following its binding to enzymes in living cells. Failure to observe lifetime kinetic changes following NADPH dehydrogenation by GR can be due to much faster kinetics of the NADPH molecule and/or much lower signal recorded in these experiments. Gathered data demonstrate the robustness of the TCSPC approach for NAD(P)H autofluorescence study directly in living cells. This approach brings an important insight into the understanding of metabolic state(s) of the heart in pathophysiological conditions.

#### Acknowledgements

Supported by CIHR (MOP 84450) grant to AC.

#### References

- [1] Benderdour M, Charron G, Comte B, et al. Decreased cardiac mitochondrial  $\text{NADP}^+$ -isocitrate dehydrogenase activity and expression: a marker of oxidative stress in hypertrophy development. *Am J Physiol Heart Circ Physiol* 2004;287:H2122-H2131.
- [2] Blinova K, Carroll S, Bose S et al. Distribution of mitochondrial NADH fluorescence lifetimes: steady-state kinetics of matrix NADH interactions. *Biochemistry* 2005;44:2585-2594.
- [3] Brautigam CA, Chuang JL, Tomchick DR, Machius M, Chuang DT. Crystal structure of human dihydrolipoamide dehydrogenase:  $\text{NAD}^+$ /NADH binding and the structural basis of disease-causing mutations. *J Mol Biol* 2005;350:543-552.
- [4] Chorvat D Jr, Chorvatova A. Spectrally resolved time-correlated single photon counting: a novel approach for characterization of endogenous fluorescence in isolated cardiac myocytes. *Eur Biophys J* 2006;36:73-83.

Address for correspondence

Dr. Chorvatova Alzbeta  
Research Center of CHU Sainte Justine, University of Montreal  
3175 Cote Sainte Catherine, H3T 1C5 Montreal, Canada  
Email. [alzbeta.chorvatova@recherche-ste-justine.qc.ca](mailto:alzbeta.chorvatova@recherche-ste-justine.qc.ca)